Journal of the American College of Cardiology
© 2008 by the American College of Cardiology Foundation
Published by Elsevier Inc.

Vol. 52, No. 10, 2008
ISSN 0735-1097/08/$34.00
doi:10.1016/j.jacc.2008.05.040

Superiority of Biphasic Over Monophasic Defibrillation Shocks Is Attributable to Less Intracellular Calcium Transient Heterogeneity

Gyo-Seung Hwang, MD, PHD,* Liang Tang, PHD,‡ Boyoung Joung, MD, PHD,‡ Norishige Morita, MD, PHD,* Hideki Hayashi, MD, PHD,* Hrayr S. Karagueuzian, PHD,† James N. Weiss, MD,† Shien-Fong Lin, PHD,‡ Peng-Sheng Chen, MD‡

Los Angeles, California; and Indianapolis, Indiana

Objectives The purpose of this study was to test the hypothesis that superiority of biphasic waveform (BW) over monophasic waveform (MW) defibrillation shocks is attributable to less intracellular calcium (Ca_i) transient heterogeneity.

Background The mechanism by which BW shocks have a higher defibrillation efficacy than MW shocks remains unclear.

Methods We simultaneously mapped epicardial membrane potential (Vm) and Ca_i during 6-ms MW and 3-ms/3-ms BW shocks in 19 Langendorff-perfused rabbit ventricles. After shock, the percentage of depolarized area was plotted over time. The maximum (peak) post-shock values (VmP and Ca_iP, respectively) were used to measure heterogeneity. Higher VmP and Ca_iP imply less heterogeneity.

Results The defibrillation thresholds for BW and MW shocks were 288 ± 99 V and 399 ± 155 V, respectively ($p = 0.0005$). Successful BW shocks had higher VmP (88 ± 9%) and Ca_iP (70 ± 13%) than unsuccessful MW shocks (VmP 76 ± 10%, $p < 0.001$; Ca_iP 57 ± 8%, $p < 0.001$) of the same shock strength. In contrast, for unsuccessful BW and MW shocks of the same shock strengths, the VmP and Ca_iP were not significantly different. The MW shocks more frequently created regions of low Ca_i surrounded by regions of high Ca_i (post-shock Ca_i sinkholes). The defibrillation threshold for MW and BW shocks became similar after disabling the sarcoplasmic reticulum (SR) with thapsigargin and ryanodine.

Conclusions The greater efficacy of BW shocks is directly related to their less heterogeneous effects on shock-induced SR Ca release and Ca_i transients. Less heterogeneous Ca_i transients reduces the probability of Ca_i sinkhole formation, thereby preventing the post-shock reinitiation of ventricular fibrillation. (J Am Coll Cardiol 2008;52:828–35)

Biphasic waveform (BW) is more effective than monophasic waveform (MW) in achieving successful defibrillation. The mechanisms underlying the superiority of BW were unclear. One hypothesis is that BW improves defibrillation efficacy by lowering the excitation threshold (1). This hypothesis, however, was not supported by subsequent studies (2,3). Kao and Hoffman (4) showed that an electrical stimulus occurring during the relative refractory period could induce graded responses and prolong action potential. It is possible that action potential (refractoriness) extension could underlie the mechanisms of defibrillation (5). If so, then BW should be more effective than MW in prolonging the refractoriness. However, Zhou et al. (6) showed that the BW shocks prolonged the action potential duration (APD) to a lesser degree than the MW shocks. Efimov et al. (7) suggested that the higher defibrillation efficacy of BW might be related to the suppression of virtual electrode-induced phase singularities in the post-shock period. In

See page 836

From the *Division of Cardiology, Department of Medicine, Cedars-Sinai Medical Center, Los Angeles, California; †Departments of Medicine (Cardiology) and Physiology, David Geffen School of Medicine at UCLA, Los Angeles, California; and the ‡Krannert Institute of Cardiology, Indiana University School of Medicine, Indianapolis, Indiana. This study was supported by the National Institutes of Health grants P01 HL78931, R01 HL78932, 58533, and 71140; the University of California Tobacco Related Disease Research Program (14IT-0001); American Heart Association Grant-in-Aid, Western States Affiliate (0255937Y and 0555057Y); a National Scientist Development Grant (0335308N); an Established Investigator Award (#0540093N); Kawata, Laubisch, Price, and Medtronic-Zipes Endowments; and a Chun Hwang Fellowship for Cardiac Arrhythmia Honoring Dr. Asher Kimchi, Los Angeles, California. Medtronic, St. Jude, and Cryocath have donated equipment to our research laboratory. Dr. Chen is a consultant to Medtronic Inc. However, this paper did not include any data on commercial products or advocate off-label use of drugs or equipment.

Manucript received December 12, 2007; revised manuscript received May 21, 2008, accepted May 27, 2008.

addition to changes of membrane potential, defibrillation shocks also have significant effects on intracellular calcium (Ca_i) transients (8). Hwang et al. (9) demonstrated that the heterogeneous distribution of Ca_i during the post-shock isoelectric window (10) plays a key role in the defibrillation outcome because the first post-shock activation always occurred from a region of low Ca_i surrounded by high Ca_i (Ca_i sinkhole). We hypothesized that MW shocks would be more likely to produce Ca_i sinkholes than BW shocks of similar strengths by creating spatially distinct virtual anodes and cathodes during the shock. Because hyperpolarization might have significantly different effects on the evolution of the Ca_i transient than depolarization, the spatially distinct virtual electrodes during an MW shock might accentuate Ca_i transient heterogeneity and facilitate the formation of Ca_i sinkholes. In contrast, during a BW shock, virtual anode formed during the first half of the shock become virtual cathode during the second half of the shock and vice versa, producing a balanced effect on sarcoplasmic reticulum (SR) Ca release. This reduced Ca_i transient heterogeneity makes the formation of Ca_i sinkholes less likely. To test this hypothesis, we compared the effects of MW and BW shocks on the 50% probability of successful defibrillation (DFT_{50}) in isolated Langendorff-perfused rabbit ventricles with dual optical mapping to record epicardial membrane potential and Ca_i simultaneously (11). We found that superiority of BW over MW was due to less Ca_i transient heterogeneity, as hypothesized.

Methods

Surgical preparation. The study protocol was approved by the Institutional Animal Care and Use Committee. New Zealand White rabbits (n = 27) weighing 5.1 ± 0.5 kg were used in this study. The hearts were perfused through aorta with Tyrode solution (sodium chloride 125, potassium chloride 4.5, sodium dihydrogen phosphate 1.8, sodium bicarbonate 24, calcium chloride 1.8, magnesium chloride 0.5, and dextrose 5.5 mmol/l, added albumin 100 mg/l in deionized water). Baseline stimulus (S_1) pacing was given to left ventricular (LV) apex. Defibrillation shocks were applied through right ventricular (RV) endocardial and LV patch electrode with direct current shocks.

Optical mapping. The hearts were stained with Rhod-2 AM and RH237 (Molecular Probes, Eugene, Oregon) and excited with laser light at 532 nm (12). In the first 25 hearts, fluorescence was collected with 2 charge-coupled device cameras (Dalsa, Waterloo, Ontario, Canada) covering the same mapped field. We used a grid to calibrate the locations of the field of view of these 2 charge-coupled device cameras. The digital images (128 × 128 pixels) were gathered from the epicardium of the LV (25 × 25 mm^2 area). We acquired 1,000 frames continuously for 4 s. The actual camera speed was calibrated by the pacing cycle length of the Bloom stimulator. The calibrated frame rate, which varied between 250 and 400 frames/s, was used for data analyses. For the last 2 hearts, we used Micam Ultima-L dual camera system (SciMedia, Costa Mesa, California) for data acquisition. There were 100 × 100 pixels/camera acquiring at 500 frames/s. Cytochalasin D (cyto-D, 5 μmol/l) was added to the perfusate to inhibit motion.

Dual optical mapping of MW and BW shocks. After 8 S_1-paced beats at 300-ms cycle length, fixed duration monophasic (6 ms) and biphasic (3 ms/3 ms) truncated exponential waveform shocks were delivered from a Ventritex (Sunnyvale, California) HVS-02 defibrillator in 19 hearts. The RV endocardial electrode was cathode, and a patch on the LV posterior wall was anode during MW shocks. During BW shocks, the first phase used LV and RV electrodes for anode and cathode, respectively. The polarity switched during the second phase. After ventricular fibrillation (VF) was induced by shock on T, an up-down algorithm was used to determine the DFT_{50}. We defined the near-threshold shock strengths as shock strengths within 50 V from the DFT_{50} (13).

Effects of ryanodine and thapsigargin. We performed 6 additional experiments to test the importance of SR Ca cycling on MW and BW shock defibrillation. The DFT_{50} was estimated before and after 30 min of perfusion with ryanodine 10 μmol/l and thapsigargin 1 μmol/l.

Shock polarity and APD. We delivered monophasic anodal shocks and cathodal shocks at 160-ms S_1-shock coupling intervals to the same defibrillation electrodes in an additional 2 hearts. The S_1 pacing cycle length was 350 ms for these 2 studies. The changes of APD throughout the mapped region were then analyzed.

Analysis of optical signals. The average fluorescence level ($\bar{F}$) over the entire 1,000 frames was first calculated for each pixel. The fluorescent level at different time points on that pixel was then compared with this average. The difference (delta) of the fluorescent level and the average fluorescence ($F - \bar{F}$) was divided by the average fluorescence ($\bar{F}$) to obtain a percentage of change above and below the average fluorescence. Shades of red and blue were used to indicate

Abbreviations and Acronyms

- **APD** = action potential duration
- **BW** = biphasic waveform
- **Ca_i** = intracellular calcium
- **Ca_iP** = the peak (maximum) area showing higher than average intracellular calcium after shock
- **Ca_iPT** = time from shock to the peak post-shock intracellular calcium
- **DFT_{50}** = shock strength associated with 50% probability of successful defibrillation
- **$\bar{F}$** = the average fluorescence level
- **LV** = left ventricular
- **MW** = monophasic waveform
- **RV** = right ventricular
- **S_1** = baseline stimulus
- **SR** = sarcoplasmic reticulum
- **VF** = ventricular fibrillation
- **VmP** = the peak (maximum) area showing simultaneous depolarization of the membrane potential after shock
- **VmPT** = time from shock to the peak area showing simultaneous depolarization of the membrane potential after shock

percentage of change above and below the average fluorescence, respectively, on the ratio maps.

Quantitative analysis of post-shock membrane potential and Ca_i changes. At each frame after shock, we determined the size (percentage) of the mapped region coded red. By default, the pixel is coded red if its fluorescence level is higher than the average (50%) fluorescence. We also performed the same analyses by coding the pixels red when the fluorescence exceeded: 1) 25% average fluorescence; and 2) 75% average fluorescence. We then plotted the percentage of frames coded red after defibrillation shocks (time 0) against time. The peak values (VmP and Ca_iP, respectively) and the time from the shock to their peak values (VmPT and Ca_iPT, respectively) were determined for each shock strength.

Previous studies showed that a near-threshold unsuccessful defibrillation shock is usually followed by synchronized repolarization (5), leading to the formation of a quiescent period during which no activation is present (13). In contrast to synchronized repolarization of membrane potential, the post-shock Ca_i changes are not synchronized, with some areas showing continued Ca_i decline, whereas the neighboring areas showed persistent Ca_i elevation. A Ca_i sinkhole is formed when a low Ca_i area is completely surrounded by a high Ca_i area (9).

Statistical analysis. All data were presented as means ± SD. Student paired *t* tests were used to compare the mean values of VmP, Ca_iP, VmPT, and Ca_iPT of the same shock strengths between MW and BW shocks ranging between 200 and 600 V. The Fisher exact test was used to compare the frequency of Ca_i sinkhole formation after MW and BW shocks. A p value of ≤ 0.05 was considered statistically significant.

Results

Unsuccessful MW shocks and successful BW shocks at equivalent shock strengths. The DFT_{50} for MW shocks was higher than for BW shocks (399 ± 155 V vs. 288 ± 99 V, p = 0.0005). In 12 hearts, we analyzed 33 pairs of shocks at the same strength in which MW shocks resulted in failed defibrillation but BW shocks resulted in successful defibrillation. Figure 1 shows a typical example comparing an unsuccessful MW shock with a successful BW shock at the same intensity. The percent areas of the mapped region with greater than average membrane potential and Ca_i levels are indicated at the top of each map.

The VmP was larger after the BW shock (76%) (Fig. 1B, panel 2) than the MW shock (66%) (Fig. 1A, panel

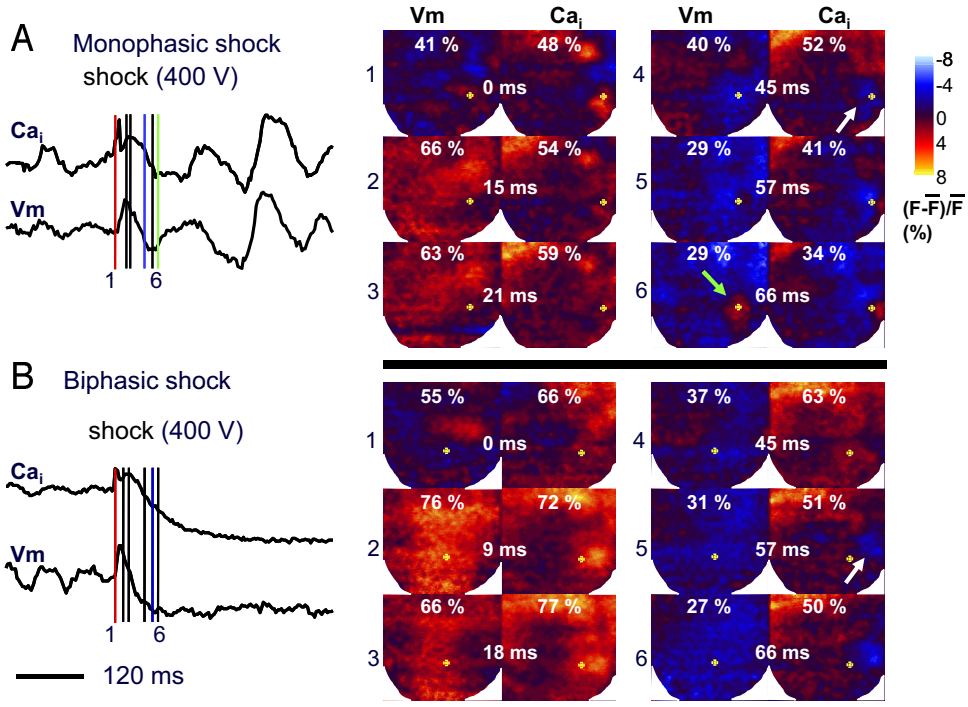

Figure 1 Dual Optical Mapping of Failed Defibrillation With Monophasic and Successful Defibrillation With Biphasic Shocks

The **left panels of A and B** show the time course of the average fluorescence of the entire mapped region after a monophasic **(upper trace)** or biphasic shock **(lower trace)**. **Right color panels** show fluorescence intensity snapshots after a failed shock (400 V) delivered at 0 ms. **Red**, **blue**, **and green line segments** indicate the time of shock, the time of intracellular calcium (Ca_i) sinkhole formation, and the end of the isoelectric window, respectively. The **yellow plus symbols** on maximum shock (Vm) maps are at the same location as the **yellow plus symbols** on the Ca_i maps. **White and green arrows** indicate Ca_i sinkhole and first post-shock activation, respectively.

2). The Ca_iP was also larger in BW than in MW (77% [Fig. 1B, panel 3] vs. 59% [Fig. 1A, panel 3]). The times between the shock and VmP (VmPT) after MW and BW shocks were 15 and 9 ms (Figs. 1A and 1B, panel 2), respectively. The times between the shock and the Ca_iP (Ca_iPT) after the MW and BW shocks were 21 and 18 ms, respectively, in these episodes (Figs. 1A and 1B, panel 3). The time of Ca_i sinkhole formation (white arrow) was 45 ms for the MW and 57 ms for BW shock (Figs. 1A and 1B, panels 4 and 5, respectively). For all 33 pairs of MW and BW shocks at the same shock strength, Ca_i sinkholes were observed in 100% of the unsuccessful MW shocks and in 64% of the successful BW shocks ($p < 0.001$). As reported in a previous study (9), the Ca_i sinkholes were not observed in type A successful defibrillation. In 13 episodes, the first post-shock activation originated from the Ca_i sinkholes within the mapped region (9). The VmP (76 ± 10% vs. 88 ± 9%, $p < 0.001$) and Ca_iP (57 ± 8% vs. 70 ± 13%, $p < 0.001$) during the isoelectric window were lower after unsuccessful MW than successful BW shocks. The VmPT was 16 ± 6 ms versus 10 ± 3 ms ($p < 0.001$), and Ca_iPT was 23 ± 6 ms versus 18 ± 4 ms ($p < 0.001$) after MW and BW shocks, respectively. Figure 2 summarizes these findings.

These results were independent of the threshold fluorescence levels used to code the pixels red. When the threshold level was 75%, the VmP for MW and BW was 25 ± 10% versus 32 ± 16%, respectively ($p = 0.015$), and the Ca_iP was 9 ± 3% and 12 ± 6%, respectively ($p < 0.001$). When the threshold level was 25%, the VmP for MW and BW was 99 ± 1% and 100 ± 1%, respectively ($p < 0.001$), and the Ca_iP was 93 ± 4% and 95 ± 4%, respectively ($p < 0.001$).

Unsuccessful BW and unsuccessful MW shocks at equivalent shock strengths. We analyzed membrane potential-Ca_i dynamics during the post-shock isoelectric window in 58 pairs (19 rabbits) of voltage-matched BW and MW shocks (354 ± 106 V) near the DFT_{50} that failed to terminate VF. In contrast to the data presented in the previous paragraph, the VmP (78 ± 9% vs. 79 ± 10%) and Ca_iP (57 ± 7% vs. 58 ± 7%) during the isoelectric window were not different after failed MW and BW shocks, respectively. However, the isoelectric window was longer

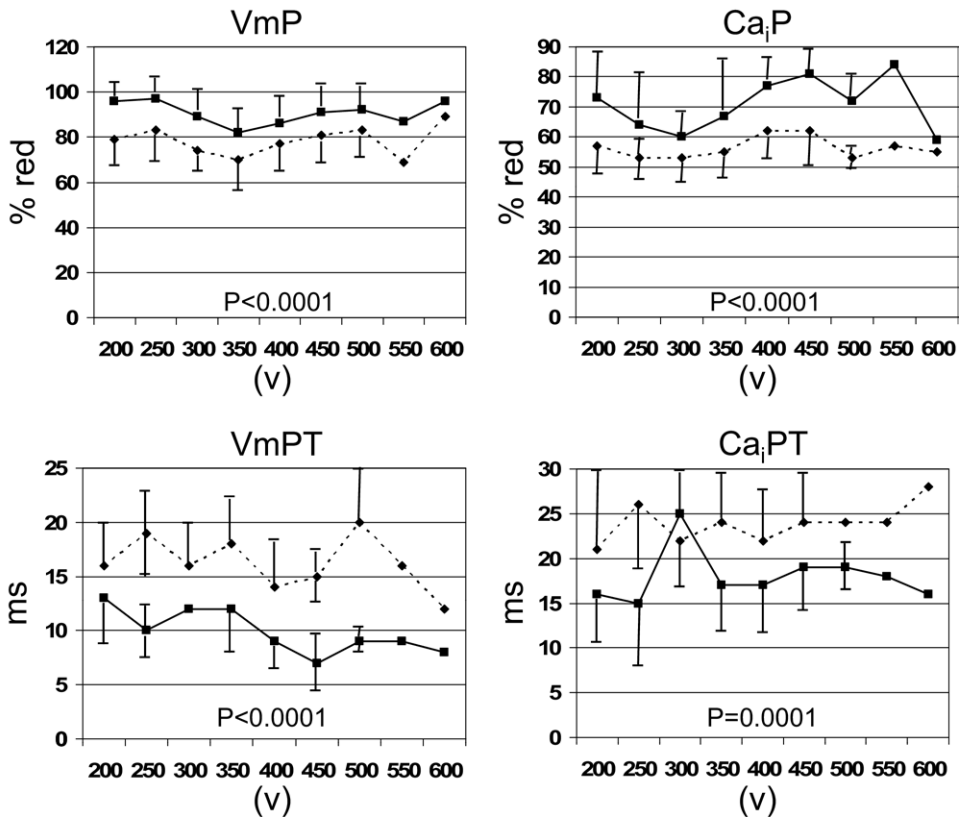

Figure 2 **Comparison Between Successful BW and Unsuccessful MW Shocks of the Same Strength**

There were significant differential effects of monophasic waveform (MW) **(diamonds)** and biphasic waveform (BW) **(squares)** shocks on the peak (maximum) area showing simultaneous depolarization of the membrane potential after shock (VmP) and the peak (maximum) area showing higher than average intracellular calcium after shock (Ca_iP), as well as time from shock to the peak area showing simultaneous depolarization of the membrane potential after shock (VmPT) and time from shock to the peak post-shock intracellular calcium (Ca_iPT).

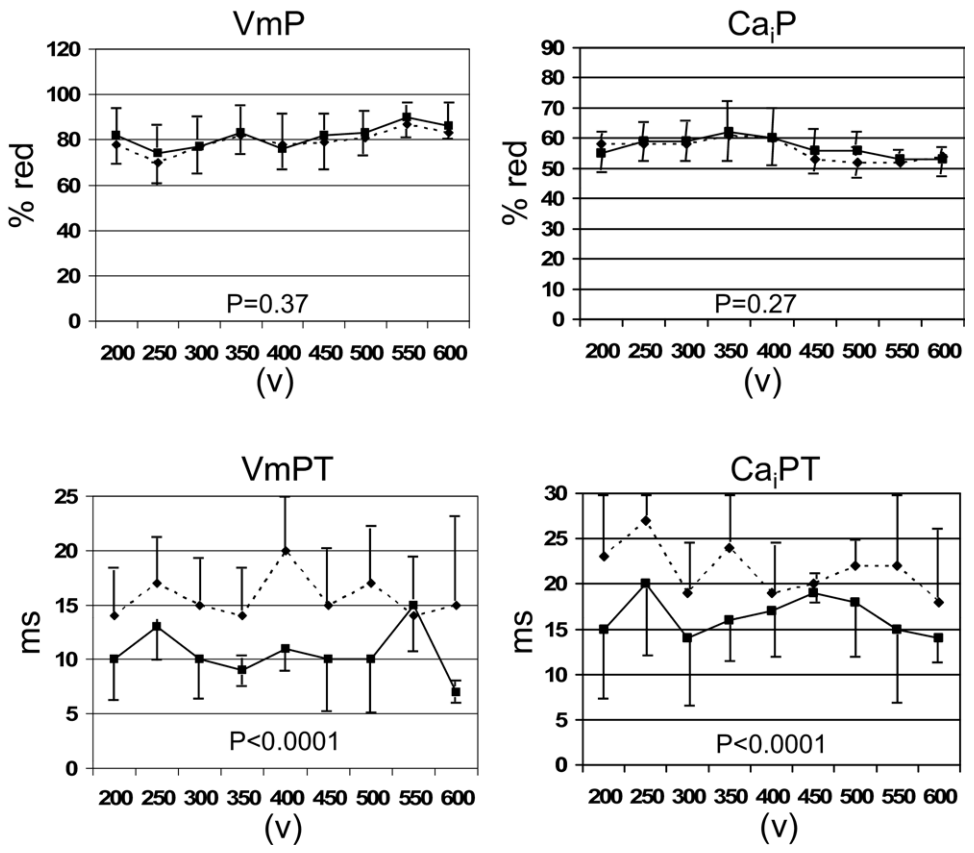

Figure 3 **Comparison Between Unsuccessful BW and Unsuccessful MW Shocks of the Same Strength**

There were no differences of VmP and Ca_iP for MW **(diamonds)** and BW **(squares)** shocks of the same strength. However, there were significant differences of VmPT and Ca_iPT. Abbreviations as in Figure 2.

after BW shocks than MW shocks (65 ± 11 ms vs. 56 ± 10 ms, respectively, $p < 0.001$). The VmPT was 16 ± 6 ms versus 11 ± 4 ms ($p < 0.001$), and for Ca_iPT it was 22 ± 7 ms versus 17 ± 6 ms ($p < 0.001$) after MW and BW shocks, respectively. Figure 3 shows these findings at different MW and BW shock strengths.

We compared 18 pairs of successful defibrillation induced by MW and BW shocks of equal strength (275 ± 90 V). We found 7 of the 18 episodes in MW shocks and 3 of 18 (p = NS) in BW shocks were type B successful defibrillation (10).

Ca_i sinkholes after MW and BW shocks. We analyzed 29 pairs (MW vs. BW) of unsuccessful defibrillation episodes in which the earliest post-shock focal activation originated from the Ca_i sinkholes. We found that the Ca_i sinkholes emerged significantly ($p = 0.02$) earlier after MW shocks (29 ± 10 ms) than after BW shocks (35 ± 11 ms) in all 29 episodes analyzed. For both MW and BW shocks, the successful defibrillation was associated with larger VmP and Ca_iP than failed defibrillation (Table 1). After ryanodine and thapsigargin, the DFT_{50} for MW and BW shocks (232 ± 42 V and 182 ± 20 V, $p = 0.02$) decreased to 165 ± 43 V and 160 ± 43 V ($p = 0.76$), respectively.

Action potential and Ca_i transient characteristics after MW versus BW shocks. Figure 4A shows that when a shock was delivered at a long coupling interval (300 ms) when repolarization was complete, MW and BW shocks had similar effects on the action potential and Ca_i transient. However, when shocks were delivered at a shorter coupling interval (160 ms) during the relative refractory period (most frequently associated with the induction of VF), BW shocks caused less prolongation of the Ca_i transient duration than MW shocks (Fig. 4B). Table 2 summarizes the results of all hearts studied. The single pixel analyses were performed by selecting a single representative pixel from the center of the mapped region. The summed fluorescence over the entire mapped region was also analyzed. We found that at the coupling interval of 160 or 140 ms, the duration of the Ca_i transient (at 70% return to baseline) was significantly shorter and more homogeneous for BW shocks than for MW shocks. The single pixel analyses showed the same trend.

Table 1 Effects of Shock Strength

	MW			BW		
	Fail	Success	p Value	Fail	Success	p Value
Voltage (V)	268 ± 98	396 ± 149		223 ± 79	318 ± 96	
VmP (%)	78 ± 14	93 ± 7	0.002	76 ± 10	91 ± 7	<0.001
VmPT (ms)	19 ± 9	14 ± 4	0.03	12 ± 4	9 ± 2	0.01
Ca_iP (%)	53 ± 5	72 ± 13	<0.001	54 ± 6	68 ± 12	<0.001
Ca_iPT (ms)	27 ± 9	21 ± 4	0.03	21 ± 6	17 ± 5	0.04
Time from shock to Ca_i sinkhole (ms)	33 ± 10	47 ± 12	0.03	24 ± 11	48 ± 16	0.02

BW = biphasic waveform; Ca_i = intracellular calcium; Ca_iP = the peak (maximum) area showing higher than average intracellular calcium after shock; Ca_iPT = time from shock to the peak post-shock intracellular calcium; MW = monophasic waveform; VmP = the peak (maximum) area showing simultaneous depolarization of the membrane potential after shock; VmPT = time from shock to the peak (maximum) area showing simultaneous depolarization of the membrane potential after shock.

Greater APD prolongation at virtual anode than virtual cathode. To further characterize the effects of virtual anodes versus cathodes on APD, we compared monophasic anodal and cathodal shocks at an S_1-shock interval of 160 ms in an additional 2 hearts. Figure 5A shows that both anodal and cathodal shocks prolonged APD at the site indicated by the arrows in Figure 5B. Figure 5B shows the formation of virtual anode and virtual cathode (arrows) during the anodal and cathodal shocks, respectively, on the epicardium near the RV endocardial electrodes. To compare the effects of shocks on APD, we subtracted the prolonged APD after the anodal shock (APD2) from that after the cathodal shock at all pixels. Figure 5C shows that in the region of the virtual electrodes there was greater prolongation of APD at anodal sites than at cathodal sites, whereas in regions surrounding the virtual electrodes, the opposite occurred. The maps of a second heart showed the same finding.

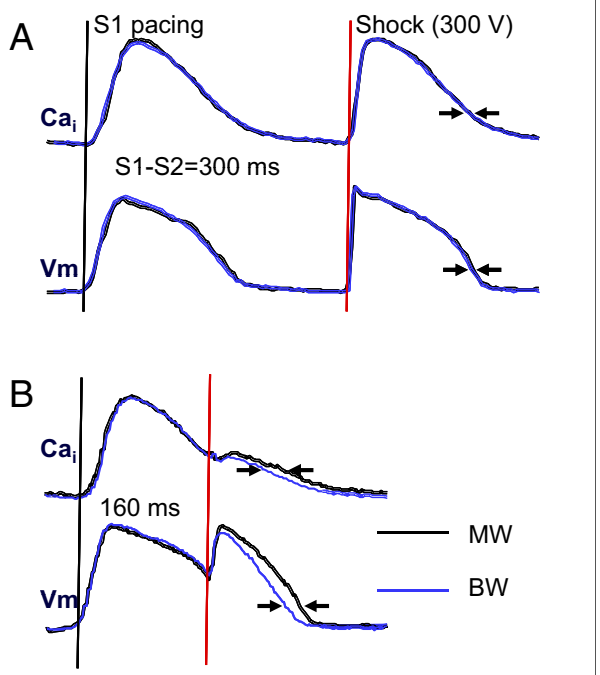

Figure 4 The Change of APD_{70} and Ca_iD_{70} After MW and BW Shocks Delivered at Different Coupling Intervals

The MW and BW shocks resulted in different action potential duration between phase 0 and 70% repolarization (APD_{70}) and Ca_iD_{70} when the coupling interval was short (160 ms) but not when the coupling interval was 300 ms. The optical signals were generated by averaging the fluorescence of the entire mapped region. Abbreviations as in Figure 2.

Discussion

In the present study, we present evidence showing that the greater efficacy of BW shocks is associated with their less heterogeneous effects on shock-induced SR Ca release and Ca_i transients.

Post-shock heterogeneity and the shock outcome. We quantified the heterogeneity by VmP and Ca_iP. A higher peak value implies a greater ability for shocks to depolarize Vm and elevate SR Ca release everywhere, reducing the Vm dispersion and the likelihood of Ca_i sinkhole formation. With this method, we found that the successful BW shocks resulted in less heterogeneous post-shock Vm and Ca_i distributions than unsuccessful MW shocks of the same strength. When both MW and BW shocks failed, there were no consistent differences between heterogeneity parameters. These findings indicate that successful defibrillation is associated with less post-shock heterogeneity.

Sources of shock-induced heterogeneity. We found that virtual anode sites were followed by larger APD prolongation than at virtual cathode sites, consistent with the hypothesis that hyperpolarization at virtual anodes increased the driving force for Ca entry through L-type Ca channels, triggering additional SR Ca release. The increased Ca_i then prolonged APD by potentiating inward Na-Ca exchange current, consistent with positive Ca_i-APD coupling (14). At virtual cathode sites, APD and Ca_i were also increased by further membrane depolarization, perhaps by reactivating recovered L-type Ca channels, but the effects were more modest. These differential APD prolongation effects were observed only in late phase 2 or 3 of the action potential but not after full repolarization. During fibrillation, the effects of virtual cathodes and

Table 2 Vm and Ca_i Changes Induced by Shock on T

	Single Representative Pixel				Summed Fluorescence Analyses			
	APD_{70} (ms)		Ca_{i70} (ms)		APD_{70} (ms)		Ca_{i70} (ms)	
CI (ms)	MW	BW	MW	BW	MW	BW	MW	BW
300	164 ± 23	163 ± 28	167 ± 23	165 ± 21	148 ± 8	147 ± 12	151 ± 13	151 ± 11
180	256 ± 45	261 ± 46	253 ± 43	256 ± 41	270 ± 38	269 ± 34	266 ± 42	265 ± 41
160	210 ± 33	206 ± 32	204 ± 35	191 ± 44*	214 ± 36	208 ± 34*	204 ± 31	197 ± 30*
140	195 ± 33	189 ± 42	182 ± 24	177 ± 21*	186 ± 18	177 ± 21*	192 ± 19	185 ± 20*

*$p < 0.05$ compared with MW.

APD_{70} = action potential duration between phase 0 and 70% repolarization; Ca_{i70} = duration of the intracellular calcium transient between the onset and 70% return to baseline; CI = coupling interval; other abbreviations as in Table 1.

anodes on APD and Ca_i transient duration are also likely to be variable depending on the local repolarization state relative to the timing of the shock. This makes it unlikely that Ca_i sinkholes would reliably form at virtual anodes or cathodes. Nevertheless, the greater efficacy of BW shocks at preventing or delaying Ca_i sinkhole formation is probably best attributed to an overall more balanced effect on the APD and the Ca_i transient, because regions that are virtual cathodes during the first half of the shock become virtual anodes during the second half of the shock and vice versa. That is, the switching between anode and cathode half-way through the shock should partially neutralize the heterogeneous effects of virtual electrodes on APD and Ca_i, hence reducing post-shock heterogeneity and improving defibrillation efficacy.

Comparison with previous studies. Raman et al. (15) have studied the effects of shocks on Ca_i, and found that the effects of shocks depend on the timing of application. Their analyses focused on the changes of Ca_i during the shock. However, Figure 2 of that report showed a greater magnitude of Ca_i elevation and APD prolongation at the virtual anode site than at the virtual cathode site. Figure 5 of the present report is consistent with their findings. Yabe et al. (16) gave shocks 300 ms after the last paced beat. Pacing studies before and after shocks showed that BW caused less conduction block than MW. Because we found no differences of Ca_i transients after BW shocks and MW shocks given 300 ms after the last paced beat, the findings of Yabe et al. (16) cannot be explained by the changes of Ca_i transients.

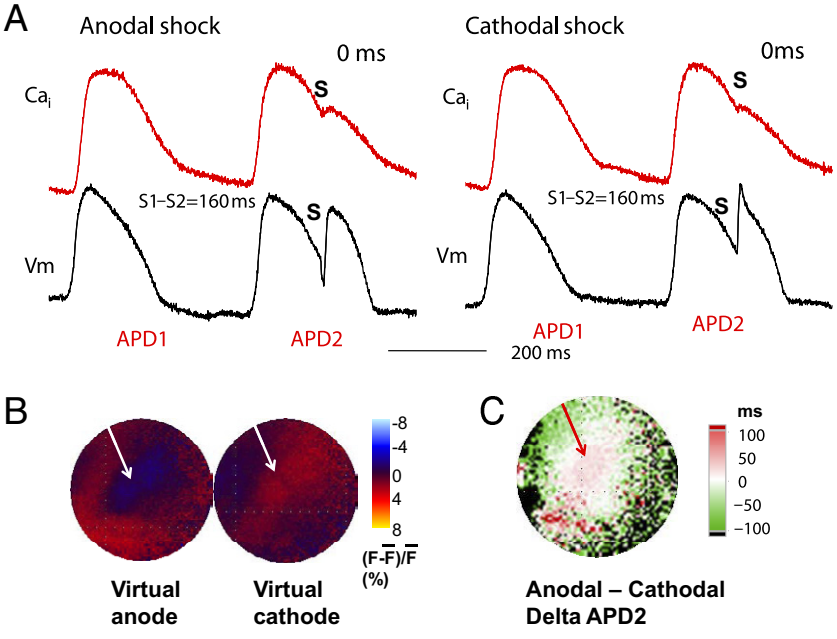

Figure 5 Delta APD and Ca_i Transient Duration Maps and Virtual Electrode Distribution During a 300 V Monophasic Shock

(A) Effects of shock (S) on the optical recordings at the sites indicated by **arrows** in **B**. **(B)** Virtual anode **(blue)** and virtual cathode **(red)** during the monophasic shocks. **(C)** Difference (delta) map between the action potential duration (APD) of the post-shock beat (APD2) constructed by subtracting APD2 of a cathodal shock from APD2 of an anodal shock. **White to red colors** indicate longer APD at the virtual anode than at virtual cathode, whereas the difference is reversed at surrounding sites. Abbreviations as in Figure 1.

Study limitations. Due to the existence of transmural heterogeneity (17), the changes in Vm and Ca_i in the intramural or subendocardial layers of the ventricles might be different than that on the epicardium. A limitation of our study is that we were not able to map the shock effects below the epicardium to determine the transmural changes of Vm and Ca_i. It is possible that the mitochondrial Ca signal influenced the recording of Ca transient. However, previous studies showed that Rhod-2 was primarily trapped in the cytosol and not in subcellular organelles such as mitochondria (11).

Summary and implications. Biphasic waveform shocks result in less spatial heterogeneity of Ca_i and delayed formation of Ca_i sinkholes, which in turn leads to delayed onset of the first post-shock activation and a longer isoelectric window compared with MW shocks. The delayed emergence of the first post-shock activation provides greater recovery time for the ventricles, thereby ensuring a higher safety factor for propagation without wavebreak. This sequence of events explains the mechanisms by which BW is more effective than MW in achieving ventricular defibrillation. We conclude that the greater efficacy of BW shocks is directly related to their less heterogeneous post-shock Ca_i transient distribution, thus reducing the probability of Ca_i sinkhole formation and VF reinitiation.

Acknowledgments

The authors thank Avile McCullen, Lei Lin, Elaine Lebowitz, and Sandra Owens for their assistance.

Reprint requests and correspondence: Dr. Peng-Sheng Chen, Krannert Institute of Cardiology, 1801 N. Capitol Avenue, E475, Indianapolis, Indiana 46202. E-mail: chenpp@iupui.edu.

REFERENCES

1. Jones JL, Jones RE, Balasky G. Improved cardiac cell excitation with symmetrical biphasic defibrillator waveforms. Am J Physiol 1987;253: H1418–24.
2. Wharton JM, Richard VJ, Murry CE, et al. Electrophysiological effects of monophasic and biphasic stimuli in normal and infarcted dogs. Pacing Clin Electrophysiol 1990;13:1158–72.
3. Daubert JP, Frazier DW, Wolf PD, Franz MR, Smith WM, Ideker RE. Response of relatively refractory canine myocardium to monophasic and biphasic shocks. Circulation 1991;84:2522–38.
4. Kao CY, Hoffman BF. Graded and decremental response in heart muscle fibers. Am J Physiol 1958;194:187–96.
5. Dillon SM. Optical recordings in the rabbit heart show that defibrillation strength shocks prolong the duration of depolarization and the refractory period. Circ Res 1991;69:842–56.
6. Zhou X, Knisley SB, Wolf PD, Rollins DL, Smith WM, Ideker RE. Prolongation of repolarization time by electric field stimulation with monophasic and biphasic shocks in open-chest dogs. Circ Res 1991; 68:1761–7.
7. Efimov IR, Cheng Y, Yamanouchi Y, Tchou PJ. Direct evidence of the role of virtual electrode-induced phase singularity in success and failure of defibrillation. J Cardiovasc Electrophysiol 2000;11:861–8.
8. Fast VG, Ideker RE. Simultaneous optical mapping of transmembrane potential and intracellular calcium in myocyte cultures. J Cardiovasc Electrophysiol 2000;11:547–56.
9. Hwang G-S, Hayashi H, Tang L, et al. Intracellular calcium and vulnerability to fibrillation and defibrillation in Langendorff-perfused rabbit ventricles. Circulation 2006;114:2595–603.
10. Chen P-S, Shibata N, Dixon EG, et al. Activation during ventricular defibrillation in open-chest dogs. Evidence of complete cessation and regeneration of ventricular fibrillation after unsuccessful shocks. J Clin Invest 1986;77:810–23.
11. Choi BR, Salama G. Simultaneous maps of optical action potentials and calcium transients in guinea-pig hearts: mechanisms underlying concordant alternans. J Physiol 2000;529:171–88.
12. Omichi C, Lamp ST, Lin SF, et al. Intracellular Ca dynamics in ventricular fibrillation. Am J Physiol Heart Circ Physiol 2004;286: H1836–44.
13. Wang NC, Lee M-H, Ohara T, et al. Optical mapping of ventricular defibrillation in isolated swine right ventricles: demonstration of a postshock isoelectric window after near-threshold defibrillation shocks. Circulation 2001;104:227–33.
14. Sato D, Shiferaw Y, Qu Z, Garfinkel A, Weiss JN, Karma A. Inferring the cellular origin of voltage and calcium alternans from the spatial scales of phase reversal during discordant alternans. Biophys J 2007; 92:L33–5.
15. Raman V, Pollard AE, Fast VG. Shock-induced changes of Ca(i)2+ and Vm in myocyte cultures and computer model: dependence on the timing of shock application. Cardiovasc Res 2007;73:101–10.
16. Yabe S, Smith WM, Daubert JP, Wolf PD, Rollins DL, Ideker RE. Conduction disturbances caused by high current density electric fields. Circ Res 1990;66:1190–203.
17. Antzelevitch C. Heterogeneity and cardiac arrhythmias: an overview. Heart Rhythm 2007;4:964–72.

Key Words: electrical stimulation ■ polarity ■ resuscitation ■ sarcoplasmic reticulum.